


 Cite this: *RSC Adv.*, 2020, 10, 17070

# Supramolecular ionogels prepared with bis(amino alcohol)oxamides as gelators: ionic transport and mechanical properties†

 Ana Šantić,<sup>a</sup> Marc Brinkkötter,<sup>b</sup> Tomislav Portada,<sup>c</sup> Leo Frkanec,<sup>c</sup> Cornelia Cremer,<sup>b</sup> Monika Schönhoff<sup>b</sup> and Andrea Moguš-Milanković<sup>a</sup>

Supramolecular ionogels composed of an ionic liquid (IL) immobilized in a network of self-assembled low-molecular weight molecules have been attracting considerable interest due to their applicability as smart electrolytes for various electrochemical applications. Despite considerable scientific effort in this field, the design of a mechanically and thermally stable yet highly conductive supramolecular ionogels still remains a challenge. In this article, we report on a series of novel ionogels of three ILs containing different cations (imidazolium/pyrrolidinium) and anions (tetrafluoroborate/bis(trifluoromethylsulfonyl)imide) prepared using (*S,S*)-bis(amino alcohol)oxamides as gelators. The gelation behaviour of the oxamide compound depends strongly on the structural features of amino alcohol substituents. Among them, (*S,S*)-bis(valinol)oxamide (capable of gelling all three ILs) and (*S,S*)-bis(phenylalaninol)oxamide (capable of gelling ILs based on bis(trifluoromethylsulfonyl)imide with a concentration as low as  $\approx 0.2$  wt%) are highly efficient. All investigated supramolecular ionogels retain the high ionic conductivity and ion diffusion coefficients of their parent IL, even for high gelator concentrations. Further, at low temperatures we observe an enhancement of the ionic conductivity in ionogels of (i) 1-butyl-3-methylimidazolium tetrafluoroborate which can be attributed to specific interactions between ionic species and gelator molecules and (ii) 1-butyl-3-methylimidazolium bis(trifluoromethylsulfonyl)imide due to inhibited crystallization. In contrast to ionic transport, mechanical strength of the ionogels shows a wider variation depending on the type and concentration of the oxamide gelator. Among all the ionogels, that of 1-butyl-3-methylimidazolium bis(trifluoromethylsulfonyl)imide prepared with 1 wt% (*S,S*)-bis(phenylalaninol)oxamide exhibits the best performance: optical transparency, stability over a wide temperature range, high conductivity and high mechanical strength. The results presented here reveal the versatile nature of bis(amino alcohol)oxamides as gelators and their high potential for preparing functionalized IL-based materials.

Received 9th February 2020

Accepted 21st April 2020

DOI: 10.1039/d0ra01249a

[rsc.li/rsc-advances](http://rsc.li/rsc-advances)

## Introduction

Supramolecular ionogels prepared by the gelation of ionic liquids (ILs) using low-molecular-weight gelators (LMWGs) are becoming increasingly important as they exhibit a unique

combination of properties which make them a superior alternative to traditional polymeric ionogels. In these versatile materials all physical properties of the parent IL (*i.e.* negligible vapor pressure, nonflammability, good electrochemical and thermal stability, high ionic conductivity) are kept preserved and additionally enriched with a solid-like consistency, self-healing capability and thermoreversible gelation property controlled by their sol-gel transition temperature.<sup>1,2</sup> In addition, LMWGs are usually biocompatible and environment-friendly<sup>3</sup> which is often not the case for polymers or inorganic particles used for gelation of ILs. All these properties make supramolecular ionogels suitable for a variety of applications from wastewater treatment,<sup>4,5</sup> medicine and pharmaceutical industry<sup>6</sup> to advanced electrochemical materials.<sup>7-11</sup> In particular, the latter field of application demands one property which is common to all supramolecular ionogels – high ionic conductivity, almost of the same value as the parent ILs. This is not the characteristic feature of polymeric ionogels, since they

<sup>a</sup>Laboratory for Functional Materials, Division of Materials Chemistry, Ruđer Bošković Institute, Bijenička c. 54, 10000 Zagreb, Croatia. E-mail: [asantic@irb.hr](mailto:asantic@irb.hr)

<sup>b</sup>Institute of Physical Chemistry, University of Muenster, Corrensstraße 28/30, 48149 Münster, Germany

<sup>c</sup>Laboratory of Supramolecular Chemistry, Division of Organic Chemistry and Biochemistry, Ruđer Bošković Institute, Bijenička c. 54, 10000 Zagreb, Croatia

† Electronic supplementary information (ESI) available: Gelators concentrations (wt%) used in preparation of ionogels from various gelator-IL combinations; Arrhenius plot of ionic conductivity for neat [C<sub>4</sub>mim][N(Tf)<sub>2</sub>] and ionogel of combination 9 with 3.0 wt% of gelator 3; spectra of the PFG-NMR diffusion measurement and echo decay data for ionogel of combination 5 with 0.5 wt% gelator; X-ray diffraction patterns for ionogels from combinations 7, 8 and 9 with 3.0 wt% of gelator 3 and gelator 3 See DOI: 10.1039/d0ra01249a



exhibit significantly lower ionic conductivity than their parent ILs.<sup>12</sup> On the other hand, supramolecular ionogels possess certain disadvantages which are mainly related to their inferior mechanical strength and low(er) temperature range of their quasi-solid state with the sol–gel transition temperature being often below 100 °C. However, recent investigations reported on supramolecular ionogels with an enhanced mechanical strength and thermal stability.<sup>13–16</sup> Such results are promising and encourage further research in the direction for finding new LMWGs, which would efficiently gel ILs producing highly conductive, however mechanically and thermally stable supramolecular ionogels.

Literature reports various LMWGs which produce gels with ILs, including those based on glycolipids,<sup>17</sup> amino acids,<sup>7,18,19</sup> sorbitol derivatives,<sup>8</sup> urea and amides,<sup>9,14</sup> cholesterol derivatives,<sup>13,20</sup> carbene complexes,<sup>21</sup> amide derivatives<sup>22–24</sup> and D-gluconic acetal derivatives.<sup>10,15</sup> Also, recent study reports preparation of the supramolecular polymeric ionogel based on the host–guest nonchemically cross-linked interactions of cyclodextrin with adamantyl derivatives.<sup>25</sup> Recently, we have reported that (*S,S*)-bis(leucinol)oxamide efficiently gels imidazolium-based IL: 1-butyl-3-methylimidazolium tetrafluoroborate, [C<sub>4</sub>mim][BF<sub>4</sub>], forming ionogels with high ionic conductivity and relatively large temperature range of the gel-state.<sup>26</sup> Most interestingly, at low concentrations of (*S,S*)-bis(leucinol)oxamide, ionogels were found to exhibit higher ionic conductivity than [C<sub>4</sub>mim][BF<sub>4</sub>] itself, which was attributed to a decrease of the electrostatic attraction between [C<sub>4</sub>mim]<sup>+</sup> and [BF<sub>4</sub>]<sup>−</sup> ions upon gelation and, consequently, their enhanced mobility. In this study we have expanded our survey to examine gelation of three ILs containing different cations and anions with a series of oxamide compounds containing different amino-alcohol groups. Results of this comprehensive study reveal certain combinations of oxamide-IL which readily form supramolecular ionogels that are highly conductive and exhibit a wide range of mechanical strength depending on the type and concentration of the gelator. Yet again, we find that the ionic conductivity of [C<sub>4</sub>mim][BF<sub>4</sub>] is enhanced upon gelation by a second oxamide gelator. Further, this study shows that the gelation of 1-butyl-3-methylimidazolium bis(trifluoromethylsulfonyl)imide, [C<sub>4</sub>mim][N(Tf)<sub>2</sub>] can inhibit the crystallization, allowing the formation of a supramolecular ionogel which is stable over a wide temperature range.

## Experimental

### Gelator synthesis and gelation tests

Enantiopure gelators: (*S,S*)-bis(leucinol)oxamide (**1**), (*S,S*)-bis(phenylalaninol)oxamide (**2**), (*S,S*)-bis(valinol)oxamide (**3**) and (*S,S*)-bis(phenylglycinol)oxamide (**4**) were prepared according to synthesis routes reported in detail in ref. 27 and 28. Ionic liquids: 1-butyl-3-methylimidazolium tetrafluoroborate – [C<sub>4</sub>mim][BF<sub>4</sub>] (≥98.5%), 1-butyl-1-methylpyrrolidinium bis(trifluoromethylsulfonyl)imide – [C<sub>4</sub>mPyr][N(Tf)<sub>2</sub>] (≥98.5%), 1-butyl-3-methylimidazolium bis(trifluoromethylsulfonyl)imide – [C<sub>4</sub>mim][N(Tf)<sub>2</sub>] (≥98%) were purchased from Sigma-Aldrich

and used as received. In gelation tests, a weighed amount of the gelator was mixed with 1 mL of IL in a test tube with a screw cap. The mixture was gently heated until the gelator dissolved and then allowed to cool to room temperature. The formation of a gel was visually checked by inversion of the test tube. The gel-forming ability was characterised quantitatively by determining the minimum gelator concentration (MGC) needed to form a gel. In order to obtain gels with varying mechanical strengths, for each ionogel combination, the concentration of gelator dissolved in IL in weight percentages was increased from MGC to 3 wt%, see Table S1 in ESI.† After preparation, the gel samples were dried in a vacuum drying system at 10<sup>−6</sup> mbar and 60 °C overnight and subsequently transferred to a glovebox.

The sol–gel transition temperature of selected ionogels was estimated visually by slowly heating the test tube in a water bath at a rate of 1 °C min<sup>−1</sup> until ionogels completely transformed into sols.

### Impedance spectroscopy

The ionic conductivity of neat ILs and prepared ionogels was measured by means of impedance spectroscopy (Novocontrol Alpha N analyzer) in the frequency range from 0.01 Hz to 1 MHz at an AC amplitude of 10 mV. For measurements, the sample was placed between two parallel gold electrodes with a Teflon ring spacer in a constant-volume cylindrical cell. To achieve complete filling of the cell, the gels were first heated above the sol–gel transition, poured into the cell and then cooled to room temperature. The measurements of all gels were performed isothermally by cooling from 20 °C to −70 °C and subsequent heating right up to 80 °C with temperature steps of 10 °C. At each temperature, samples were thermally equilibrated for at least 50 min prior to the measurement. In order to check the reliability of the results of ionic conductivity measurements, each ionogel sample was measured three times under identical experimental conditions.

### PFG-NMR

Pulsed-field-gradient NMR (PFG-NMR) measurements were performed using an Avance III HD 400 MHz spectrometer (Bruker) with a permanent field strength of 9.4 T. The gradient probe head ‘Diff50’ (Bruker) was used with selective radio frequency inserts for <sup>1</sup>H and <sup>19</sup>F. The temperature was controlled using a GMH 3710 controller with a PT100 thermocouple (Greisinger electronics, Germany). The samples were filled into the NMR tubes inside a glove box and the tubes were evacuated and then ablated.

A stimulated echo pulse sequence with field gradient pulses was applied to measure the self-diffusion coefficients.<sup>29</sup> The self-diffusion coefficients *D* were calculated by eqn (1)

$$I(g) = I(0)\exp(-bD) = I(0)\exp\left(-\gamma^2 g^2 \delta^2 D \left(\Delta - \frac{\delta}{3}\right)\right) \quad (1)$$

where *b* is defined by eqn (1),  $\delta$  is the gradient pulse duration, *g* the gradient strength, and  $\Delta$  the observation time between two gradient pulses. In a series of spectra, *g* was incremented

stepwise in order to vary  $b$ , and respective peak intensities were evaluated to yield  $I(g)$ .

### Rheology

The complex shear modulus of ionogels was measured at 20 °C in a frequency range from 0.01 Hz to 15 Hz using a MCR 101 rheometer (Anton Paar). A cone-plate configuration of 25 mm diameter and 1° cone angle was used for all measurements. Complex viscosity spectra were collected in an auto-stress mode, in which the stress value is automatically adjusted during the measurement to maintain a constant strain. Strain values, within the linear viscoelastic response range, were determined in a preliminary strain sweep experiment. All ionogels show linear viscoelastic behaviour below the strain value of 0.01 ( $\gamma = 1\%$ ).

### X-ray diffraction measurements

XRD measurements of selected ionogels and gelators were performed on a PANalytical Aeris X-ray diffractometer with Ni-filtered Cu K $\alpha$  radiation.

## Results and discussion

### Gelation properties of oxamide-based gelators towards ILs

The gelation tests of combinations of four gelators with three ILs show that (*S,S*)-bis(valinol)oxamide (**3**) is the most efficient gelator capable to gel all selected ILs, see Table 1. However, in terms of gelation propensity, the most effective gelator is (*S,S*)-bis(phenylalaninol)oxamide (**2**) which gels [C<sub>4</sub>mPyr][N(Tf)<sub>2</sub>] and [C<sub>4</sub>mim][N(Tf)<sub>2</sub>] with a minimum gelator concentration (MGC) as low as 0.2 wt% and 0.3 wt%, respectively. For all other ionogels, the MGC is found to vary from 0.5 wt% to 1.7 wt%, see Table 1.

Considering the substituents on the oxamide unit, it is remarkable to observe that very small differences in their structure strongly influence gelation behaviour towards ILs, compare for example gelators **1** and **3**, as well as **2** and **4**. In general, oxamide-based gelators appear to be very efficient gelators for various organic solvents and water.<sup>27,28,30</sup> It is known that their gelation ability is the result of strong and directional intermolecular hydrogen bonding provided by oxamide units and the lack of a plane of symmetry due to the presence of two chiral centres of identical configuration, which is known to prevent crystallization and favours aggregation.<sup>27,28,30</sup> Our recent computational investigation<sup>26</sup> of the interactions between (*S,S*)-bis(leucinol)oxamide (**1**) and [C<sub>4</sub>mim][BF<sub>4</sub>] revealed that the oxamide unit has two times larger affinity towards the [BF<sub>4</sub>]<sup>-</sup> anion than for the [C<sub>4</sub>mim]<sup>+</sup> cation. The former interaction is established through four hydrogen bonds involving two fluorine atoms in [BF<sub>4</sub>]<sup>-</sup> and all four acidic hydrogen atoms of the gelator. In the [gelator **1**][BF<sub>4</sub>]<sup>-</sup> complex, the carbonyl groups of the neighbouring amide fragments adopt a *syn* conformation which maximizes the number of available hydrogen-bond donors towards [BF<sub>4</sub>]<sup>-</sup>. In that study,<sup>26</sup> we modelled the [gelator **1**][C<sub>4</sub>mim][BF<sub>4</sub>] complex with a terminal -CH<sub>3</sub> group instead of the -CH<sub>2</sub>CH(CH<sub>3</sub>)<sub>2</sub> moiety in gelator **1**. Basically, this model

could also work for other gelators (**2–4**) in this study in combination with [C<sub>4</sub>mim][BF<sub>4</sub>]; however, their different gelation behaviour reveals that the substituent groups have a strong influence on the gelation process, see combinations **1**, **4**, **7** and **10** in Table 1. For instance, gelators **1** and **3** containing similar substituents exhibit a significant difference in the minimum concentration needed to gel [C<sub>4</sub>mim][BF<sub>4</sub>]. Here, it can be inferred that a longer -CH<sub>2</sub>CH(CH<sub>3</sub>)<sub>2</sub> substituent which is structurally more flexible allows better interaction between acidic hydrogen atoms of the gelator and [BF<sub>4</sub>]<sup>-</sup> ions than a shorter and more rigid -CH(CH<sub>3</sub>)<sub>2</sub> moiety, which sterically hinders this interaction thus causing lower gelator efficiency. The steric effect could also be the reason for extremely slow gelation dynamics of gelators **2** and **4**, both containing large rigid phenyl rings, to form gel with [C<sub>4</sub>mim][BF<sub>4</sub>], see Table 1. In fact, both gelators do form ionogels with [C<sub>4</sub>mim][BF<sub>4</sub>], but with a very long gelation time (>12 h), which makes characterization of this material difficult and its application potential limited. Further, the effect of steric hindrance on the gelation, which is expected to be the largest in gelator **4** due to a close distance between an aromatic ring and acidic hydrogen atoms, could explain the lowest gelation ability of this gelator towards all ILs.

On the other hand, high efficiency of gelators **2** and **3** in gelation of [C<sub>4</sub>mPyr][N(Tf)<sub>2</sub>] and [C<sub>4</sub>mim][N(Tf)<sub>2</sub>] is most probably related to the interactions with the [N(Tf)<sub>2</sub>]<sup>-</sup> anion, see Table 1. In particular, it is interesting to note that gelator **2**, which exhibits very slow gelation of [C<sub>4</sub>mim][BF<sub>4</sub>], is especially efficient for both ILs containing [N(Tf)<sub>2</sub>]<sup>-</sup> anion. This points to the favourable interactions of the [N(Tf)<sub>2</sub>]<sup>-</sup> anion and hydrogen atoms from the gelator **2** without a significant steric effect of the phenyl ring. However, for drawing any further conclusions on the interactions between oxamide gelators and ILs containing [N(Tf)<sub>2</sub>]<sup>-</sup> anion and their implications on the gelation mechanisms it is necessary to include molecular dynamics simulations and quantum mechanical calculations. These studies are under way.

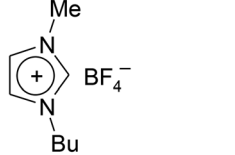
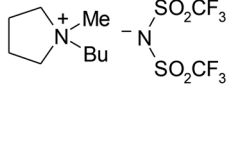
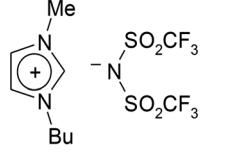
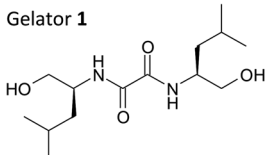
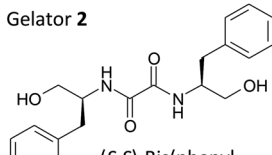
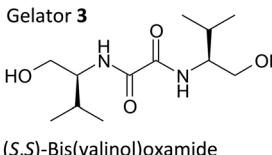
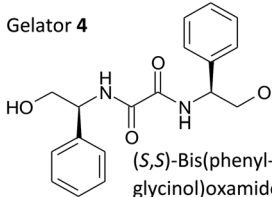
The sol-gel transition temperatures of the ionogels at the MGC are within the range from 55 °C to 65 °C and increase with increasing gelator concentration up to 3 wt% to about 85 °C to 95 °C, depending on the gelator compound. A complete list of the concentrations of gelators used for preparation of ionogels from different combinations is given in Table S1 in ESI.†

### Ionic transport

As mentioned earlier in the Introduction, supramolecular ionogels are well-known for their high ionic conductivity, being almost of the same value as the parent IL. This is also true for all ionogels in the present study. Fig. 1 shows the ionic conductivity measured at 20 °C for the neat ILs and their corresponding ionogels as a function of gelator concentration. It is clearly visible from Fig. 1 that for all three ILs, gelation has practically no influence on the ionic conductivity at 20 °C even at higher gelator concentrations.

The presented results are remarkable in two aspects. First, in our previous study of ionogels from the combination **1** we found that the samples with low gelator concentrations have somehow

Table 1 Combinations of oxamide-based gelators and ionic liquids

Ionic liquids Oxamide gelators	 1-Butyl-3-methylimidazolium tetrafluoroborate $[C_4mim][BF_4]$	 1-Butyl-1-methylpyrrolidinium bis(trifluoromethylsulfonyl)imide $[C_4mPyr][N(Tf)_2]$	 1-Butyl-3-methylimidazolium bis(trifluoromethylsulfonyl)imide $[C_4mim][N(Tf)_2]$
Gelator 1  (S,S)-Bis(leucinol)oxamide	Combination 1 IONOGEL <sup>26</sup> MGC <sup>a</sup> : wt $\approx$ 0.7%	Combination 2 IONOGEL (opaque) MGC: wt $\approx$ 0.5%	Combination 3 No gelation Opaque solution
Gelator 2  (S,S)-Bis(phenylalaninol)oxamide	Combination 4 IONOGEL <sup>b</sup> (opaque) – long gelation time	Combination 5 IONOGEL (transparent) MGC: wt $\approx$ 0.2%	Combination 6 IONOGEL (transparent) MGC: wt $\approx$ 0.3%
Gelator 3  (S,S)-Bis(valinol)oxamide	Combination 7 IONOGEL (opaque) MGC: wt $\approx$ 1.7%	Combination 8 IONOGEL (opaque) MGC: wt $\approx$ 0.7%	Combination 9 IONOGEL (opaque) MGC: wt $\approx$ 0.7%
Gelator 4  (S,S)-Bis(phenylglycinol)oxamide	Combination 10 IONOGEL <sup>b</sup> (opaque) – long gelation time	Combination 11 No gelation Transparent solution	Combination 12 No gelation Transparent solution

<sup>a</sup> MGC – minimum gelator concentration. <sup>b</sup> For combinations 4 and 10 the formation of a stable ionogel is observed after approximately 12 hours of leaving the solution at rest at room temperature. These systems were not further analysed.

higher ionic conductivity than the neat IL.<sup>26</sup> This effect was found to be weak at room temperature, but with decreasing temperature it becomes pronounced and finally at  $-70\text{ }^\circ\text{C}$  ionogels are almost one order of magnitude more conductive than the parent  $[C_4mim][BF_4]$ . Now the question arises whether the gelation of  $[C_4mim][BF_4]$  with gelator 3 produces a similar effect. Indeed, we find that at  $20\text{ }^\circ\text{C}$  most of ionogels from the combination 7 show slightly higher conductivity (see the left panel in Fig. 1). Furthermore, as temperature decreases, their ionic conductivity gets progressively higher than the conductivity of the neat  $[C_4mim][BF_4]$ , see Fig. 2. It is therefore reasonable to assume that the increase in ionic conductivity upon gelation with gelator 3 has a similar origin as in the case of gelator 1, *i.e.* higher mobility of ionic species as a consequence

of the reduced electrostatic attraction between  $[C_4mim]^+$  and  $[BF_4]^-$  due to higher affinity of the gelator molecules towards the  $[BF_4]^-$  ions.

Second, in our previous study a reverse effect is observed at higher concentrations of gelator 1 ( $\geq 3\text{ wt}\%$ ), as these ionogels exhibit somehow smaller ionic conductivity than the parent  $[C_4mim][BF_4]$ .<sup>26</sup> The reason for this is most likely a denser gelator matrix which hinders the pathways for ionic transport.<sup>26</sup> For ionogels from combination 7 such a decrease is not observed up to 3 wt% of gelator concentration, see Fig. 1 and also Fig. 2 for higher temperatures. This is most probably because the gelator concentration of 3 wt% is not large enough to form a dense gelator matrix capable to produce this effect (note that 3 wt% of gelator in combination 1 is 4.3 times larger

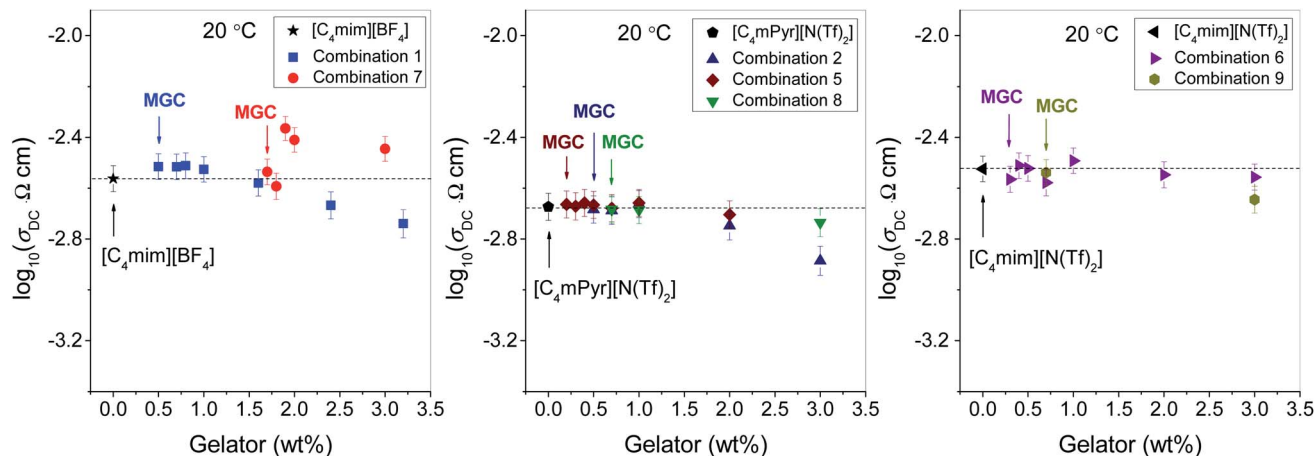


Fig. 1 Ionic conductivity measured at 20 °C of parent ionic liquids and their corresponding ionogels as a function of gelator concentration.

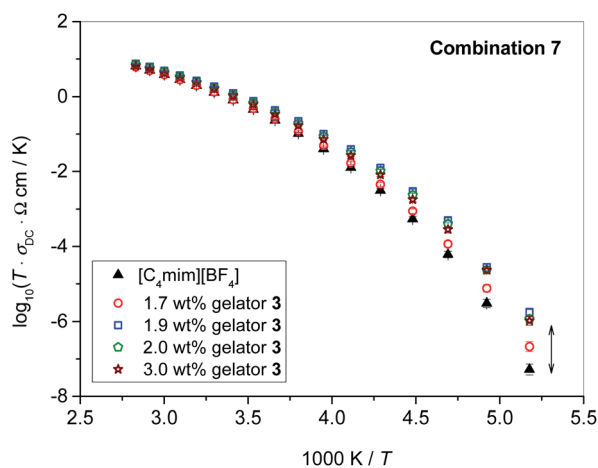


Fig. 2 Ionic conductivity as a function of reciprocal temperature for neat  $[C_4mim][BF_4]$  and ionogels from combination 7 with various concentrations of gelator 3. The error bars are at most of the order of the symbol size.

than the MGC, whereas in the case of combination 7 it is only 1.8 times larger than the corresponding MGC). Similarly, for gelator 2 the ionic conductivity of the ionogels from combinations 5 and 6 prepared with 3 wt% of gelators is also very similar to that of the neat ILs despite much higher ratio of gelator concentrations (note that 3 wt% of gelator in combination 5 is 15 times larger than the MGC). This result suggests significant difference in the structural features of the gelator network in these ionogels as compared to combination 1. Indeed, the ionogels from combination 5 and 6 are optically transparent, which suggests that their structures comprise very small gelator aggregates, too small to scatter visible light. Therefore, it is likely that their fine gelator network formed even at very high gelator concentration allows unrestricted ionic transport resulting in high ionic conductivity of these ionogels.

In contrast to  $[C_4mim][BF_4]$  which exhibits non-Arrhenius temperature dependence of conductivity down to glass transition,  $T_g \approx -85$  °C, which is typical for a fragile melt, the two

other ILs containing imide anion, namely  $[C_4mPyr][N(Tf)_2]$  and  $[C_4mim][N(Tf)_2]$ , display a tendency to crystallize below  $-30$  °C and  $-40$  °C, respectively. The crystallization manifests as an instantaneous drop in ionic conductivity of the IL, see Fig. 3. However, while ionogels formed of  $[C_4mPyr][N(Tf)_2]$  and gelators 1–3 are also prone to crystallization, the crystallization of  $[C_4mim][N(Tf)_2]$  is prevented by gelation with gelator 2 as can be seen in Fig. 3. Similar findings were also observed for gelator 3, see Fig. S1 in ESI.† Although crystallization of  $[C_4mim][N(Tf)_2]$  can be avoided by simple annealing protocols,<sup>31</sup> the above result is beneficial since these ionogels show good stability in cooling and heating cycles in a wide temperature range (down to  $-80$  °C) without applying any pre-treatments.

Similarly as for ionic conductivity, cationic and anionic diffusion coefficients were measured at 20 °C in all ionogels, and compared to the respective parent ILs, see Fig. 4. For all ILs, we found that cations (open symbols in Fig. 4) diffuse faster

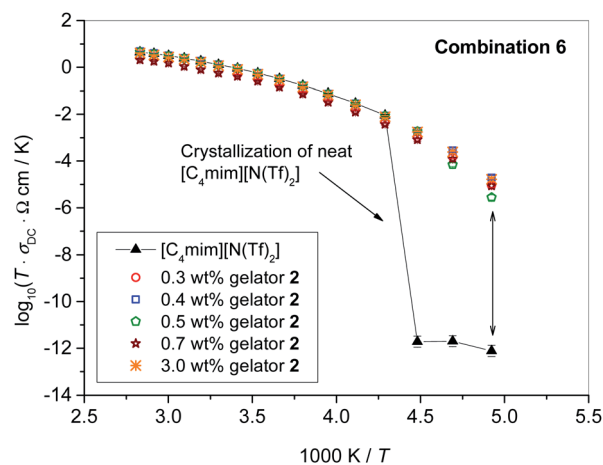


Fig. 3 Ionic conductivity as a function of reciprocal temperature for neat  $[C_4mim][N(Tf)_2]$  and ionogels of combination 6 with various concentrations of gelator 2. The line connecting the data for  $[C_4mim][N(Tf)_2]$  is a guide to the eye. The error bars are at most of the order of the symbol size.

than anions (full symbols), which is in accordance to the literature.<sup>32–34</sup> This trend is also preserved in all ionogels in this study. Moreover, within error the values of the diffusion coefficients remain the same as those of the parent ILs, indicating negligible influence of gelation on the mobility of cations and anions of the IL at 20 °C. This is in line with their high ionic conductivity over a wide range of gelator concentrations discussed above.

It is of further interest to investigate the diffusive behaviour of the gelator itself, as this might provide information about the mechanism of stabilization. The gelator concentration is very low, and in a one-pulse <sup>1</sup>H spectrum its signal is superimposed on cation resonances. However, in a PFG diffusion experiment it is possible to make use of the rapid decay of the cation signals, and observe the decay of the gelator signal at very high gradient strengths, see spectra in the ESI, Fig. S2.† This proves a very slow diffusion of the gelator. A quantitative evaluation by a fit of the gelator signal only is given in Fig. S3† for combination 5 at 0.5 wt% of gelator 2. This results in a diffusion coefficient of  $D_{\text{Gelator}} = 1.7 \times 10^{-12} \text{ m}^2 \text{ s}^{-1}$ , which is about one order of magnitude lower than the cation or anion diffusion (compare to the middle panel in Fig. 4). It is thus proven that the gelator is mobile too, however, far less than the ionic components.

## Rheological properties

While the ionic transport of ILs is mostly unaffected by the gelation process or even enhanced in the case of  $[\text{C}_4\text{mim}][\text{BF}_4]$ , the rheological properties significantly differ depending on the oxamide gelator and its concentration. Fig. 5 shows the frequency dependence of storage modulus ( $G'$ ) and loss modulus ( $G''$ ) of the combination 5 ionogel containing 0.5 wt% of gelator 2. Both moduli are nearly frequency-independent over the investigated frequency range, with  $G'$  (the contribution of elastic, solid-like behaviour and thus a measure of the mechanical strength) being one order of magnitude higher than  $G''$  (the contribution of viscous, liquid-like behaviour), indicating typical supramolecular gel behaviour.<sup>35,36</sup>

Other ionogels in this study show similar rheological properties in terms of frequency-independent viscoelastic quantities and their relation,  $G' > G''$ , however, the absolute magnitudes of storage and loss moduli are very different for different ionogels. Fig. 6 displays values of  $G'$  and  $G''$  at 0.1 Hz and 20 °C for different ionogel combinations as a function of gelator concentration normalized by the respective MGC.

From this figure two observations are evident. First, at the MGC, storage modulus of the ionogels of the *same* IL significantly varies depending on the gelator compound (see grey areas in Fig. 6). For instance, gelation of  $[\text{C}_4\text{mim}][\text{N}(\text{Tf})_2]$  by gelator 2 (combination 6) produces significantly stronger gels than that by gelator 3 (combination 9) as evidenced by almost three order of magnitude higher storage modulus at the MGC, see the right panel in Fig. 6. In the case of  $[\text{C}_4\text{mPyr}][\text{N}(\text{Tf})_2]$ , gelation by gelator 2 (combination 5) and 3 (combination 8) produces mechanically stronger gels than by gelator 1 (combination 2), see the middle panel in Fig. 6. Also, gelator 3 forms a rather weak ionogel with  $[\text{C}_4\text{mim}][\text{BF}_4]$  (combination 7), see the left panel in Fig. 6.

Second, ionogels exhibit a different evolution of viscoelastic properties with the increase of the concentration of the gelator. It can be observed that  $[\text{C}_4\text{mPyr}][\text{N}(\text{Tf})_2]$  gelled by gelator 1 and 2

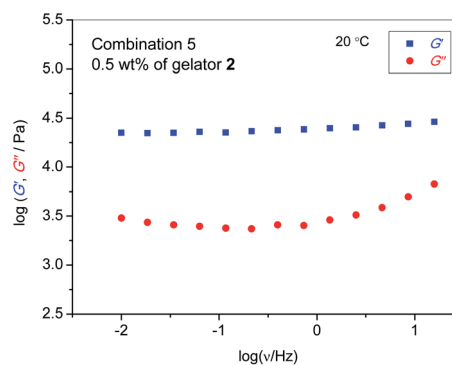


Fig. 5 Storage ( $G'$ ) and loss modulus ( $G''$ ) of an ionogel from combination 5 with 0.5 wt% of gelator 2.

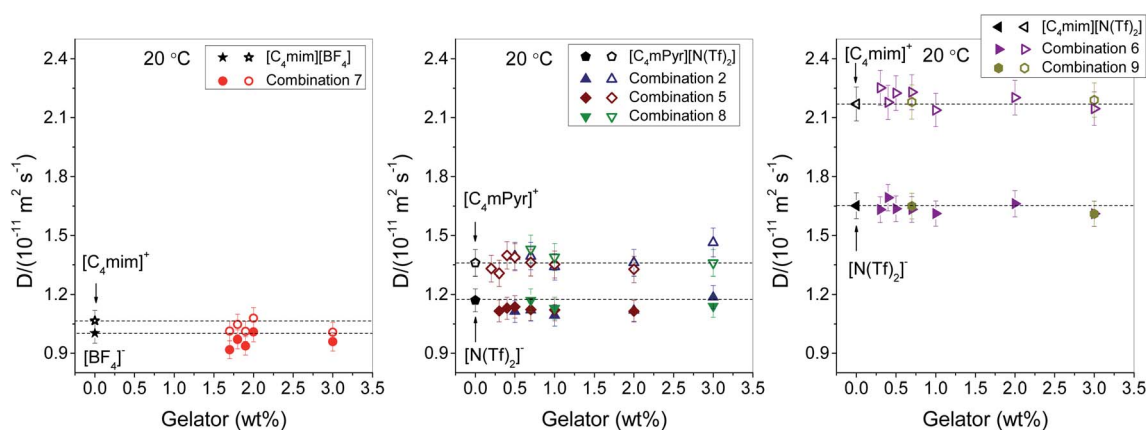


Fig. 4 Diffusion coefficients of cations and anions at 20 °C for the neat ionic liquids and ionogels of various combinations as a function of gelator concentration. Open symbols: cation; full symbols: anion.

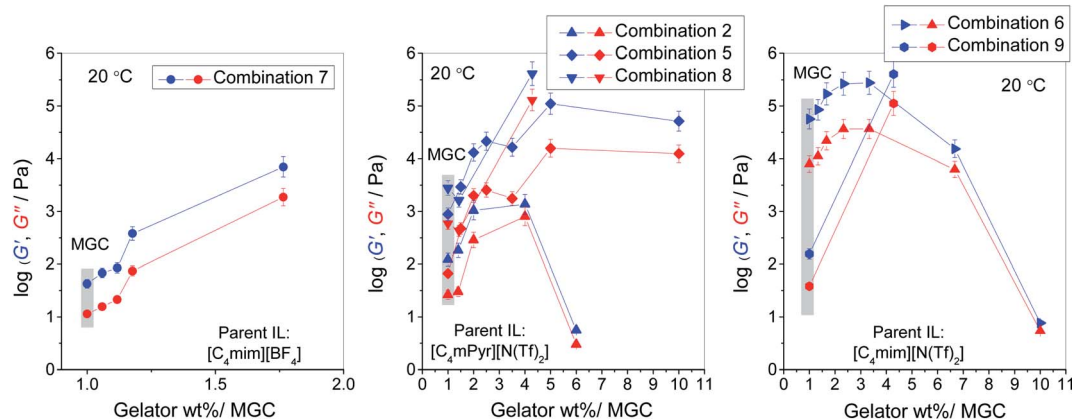


Fig. 6 Storage ( $G'$ ) and loss ( $G''$ ) modulus at 20 °C of various ionogels as a function of gelator concentration normalized by the MGC. Blue symbols:  $G'$ , red symbols:  $G''$ . Lines are guides to the eye.

as well as  $[C_4\text{mim}][\text{N}(\text{Tf})_2]$  gelled by gelator 2 show a non-linear increase of  $G'$  with increasing gelator concentration with a maximum at approximately a concentration 3 times higher than the MGC. The maximal value of  $G'$  indicates the optimal gelator concentration for which the mechanically strongest ionogel is formed, whereas, a further decrease in  $G'$  reveals destabilisation of the gel structure, probably due to excess of gelator molecules which do not participate in self-assembly. Indeed, for the most concentrated ionogels relative to MGC (especially combinations 2 and 6) the values of  $G'$  and  $G''$  almost converge, suggesting an ease of breakage of the gelator matrix and transition to more liquid-like behaviour. On the other hand, ionogels of all three ILs formed with gelator 3 (combination 7, 8 and 9) show a continuous increase in  $G'$  and  $G''$  with a gelator concentration indicating steady strengthening of the ionogel structure. At highest gelator concentration (3 wt%), these three ionogels contain small solid particles which are detectable in a gap adjustment in rheological measurements. The XRD pattern for these ionogels shows small diffraction peaks superimposed on a strong background halo confirming the traces of crystalline gelator in an amorphous gel, see Fig. S4 in ESI.† Since the crystalline gelator particles are dispersed in these gels in very small amounts, they have no influence on the ionic conductivity of these materials which remains high.

Interestingly, optically transparent ionogels from combination 5 and 6 are characterised by the highest mechanical strengths among all samples. This indicates that their gel networks have larger number of the stress-bearing strands, therefore, resulting in a highly elastic material. Indeed, storage modulus for the ionogel from the combination 6 containing 1 wt% of gelator 2 (optimal gelator concentration) reaches 278 kPa, which is higher than that of the strongest ionogel prepared by gelators based on urea ( $\approx 160$  kPa),<sup>13</sup> and that of highly temperature-stable ionogels prepared *via* metal-coordination interaction ( $\approx 46$  kPa).<sup>15</sup>

Interestingly, such high mechanical strength is achieved in spite of the high gelator mobility ( $D_{\text{Gelator}}$  on the order of  $10^{-12}$   $\text{m}^2 \text{s}^{-1}$ ). Clearly, aggregation of gelator molecules with anions plays a major role, as discussed above, and this aggregation is responsible for the mechanical stability. The aggregates, are,

however, highly flexible, allowing molecular exchange and thus displacements of gelator molecules. The lifetime  $t$  of a gelator molecule in a stress-bearing strand is shorter than the observation time in the PFG experiment, *i.e.* it can be estimated as  $t < 100$  ms.

In summary, it is remarkable to observe that while mechanical strength of various supramolecular ionogels in this study spans four orders of magnitude ( $G' \approx 42$  Pa to 278 kPa) their transport properties remain the same as of the parent ILs, compare Fig. 1, 4 and 6. This result implies that the network architecture of the self-assembled bis(amino alcohol)oxamide molecules has little influence on the transport properties of the ILs inside these ionogels. Unlike in polymer ionogels, ionic transport in these materials is completely decoupled from the mechanical relaxation. This unique property offers a vast range of opportunities for a design of highly conducting material with tuneable mechanical properties. In particular, the combination of high ionic conductivity, high mechanical strength, thermoreversible gelation property and a wide temperature range of quasi-solid state makes these ionogels especially attractive as electrolytes in solar cells<sup>9</sup> and solid state batteries.

## Conclusions

The efficient gelation of the three ILs containing different cations (imidazolium/pyrrolidinium) and anions (tetrafluoroborate/bis(trifluoromethylsulfonyl)imide) has been achieved using low-molecular weight bis(amino alcohol)oxamides. A comparative gelation test reveals that (*S,S*)-bis(valinol)oxamide is the most efficient gelator capable to gel all three ILs, whereas (*S,S*)-bis(phenylalaninol)oxamide exhibits the best gelation potential towards ILs containing a bis(trifluoromethylsulfonyl)imide anion. Based on correlations between the structures of the gelators and ILs it can be inferred that the steric effect, which depends on the size and flexibility of the amino alcohol substituents on the oxamide unit, plays a key role in the gelation process. All prepared ionogels show a high ionic conductivity implying that the gelator matrix does not hinder transport of cations and anions of the IL.

In fact, studying ionic conductivity in a temperature range down to the IL's  $T_g$ , we find two cases in which the gelation has a *positive* effect on ionic transport. The first case refers to the ionogels of  $[C_4mim][BF_4]$  prepared by gelation with (*S,S*)-bis(leucinol)oxamide and (*S,S*)-bis(valinol)oxamide in which interactions among gelator molecules and ionic species result in a higher mobility of ions and hence, facilitate ionic transport. The second one is related to the ionogels of  $[C_4mim][N(Tf)_2]$  formed by gelation with (*S,S*)-bis(phenylalaninol)oxamide and (*S,S*)-bis(valinol)oxamide where gelation indirectly increases ionic conductivity at low temperatures by preventing crystallization of the IL.

On the other hand, mechanical strength of the prepared ionogels spans four orders of magnitude and shows a strong dependence on the gelator type and concentrations indicating that the ionic transport is completely decoupled from the mechanical relaxation in these materials. Taking into account all above reported properties, we find that ionogel with the best performance properties is obtained when  $[C_4mim][N(Tf)_2]$  is gelled with 1 wt% of (*S,S*)-bis(phenylalaninol)oxamide. This ionogel is optically transparent, stable over a wide temperature range ( $-70\text{ }^\circ\text{C}$  to  $80\text{ }^\circ\text{C}$ ), highly conductive ( $0.0032\text{ }(\Omega\text{ cm})^{-1}$  at  $20\text{ }^\circ\text{C}$ ) and mechanically strong ( $G' = 278\text{ kPa}$  at  $20\text{ }^\circ\text{C}$ ). Overall, these results provide a guidance for further development of functional ionogels using oxamide gelators.

## Conflicts of interest

There are no conflicts to declare.

## Acknowledgements

This work was supported by the Croatian-German bilateral project (MZOS-DAAD) "Development of novel supramolecular ionogels for advanced electrolytes" and the donation from the Croatian Academy of Science and Arts (HAZU). MB was supported by a stipend of the "Fonds der Chemischen Industrie" (FCI, Germany). TP and LF acknowledge the financial support of the Croatian Science Foundation, Project: IP-2018-01-6910: "Synthesis of Supramolecular Self-assembled Nanostructures for Construction of Advanced Functional Materials". The authors are pleased to acknowledge Vilko Mandić (Faculty of Chemical Engineering and Technology, University of Zagreb, Croatia) and Ivan Halasz (Laboratory for Green Synthesis, Division of Physical Chemistry, Ruđer Bošković Institute, Croatia) for performing XRD measurements.

## References

- 1 P. C. Marr and A. C. Marr, *Green Chem.*, 2016, **18**, 105.
- 2 J. Le Bideau, L. Viau and A. Vioux, *Chem. Soc. Rev.*, 2011, **40**(2), 907.
- 3 B. O. Okesola and D. K. Smith, *Chem. Soc. Rev.*, 2016, **45**, 4226.
- 4 C. Rizzo, S. Marullo, P. R. Campodonico, I. Pibiri, N. T. Dintcheva, R. Noto, D. Milan and F. D'Anna, *ACS Sustainable Chem. Eng.*, 2018, **6**(9), 12453.
- 5 S. Dutta, D. Das, A. Dasgupta and P. K. Das, *Chem.–Eur. J.*, 2010, **16**, 1493.
- 6 C. Rizzo, R. Arrigo, N. T. Dintcheva, G. Gallo, F. Giannici, R. Noto, A. Sutera and P. Vitale, *Chem.–Eur. J.*, 2017, **23**(64), 16297.
- 7 W. Kubo, S. Kambe, S. Nakade, T. Kitamura, K. Hanabusa, Y. Wada and S. Yanagida, *J. Phys. Chem. B*, 2003, **107**, 4374.
- 8 N. Mohmeyer, P. Wang, H.-W. Schmidt, S. M. Zakeeruddin and M. Grätzel, *J. Mater. Chem.*, 2004, **14**, 1905.
- 9 N. Mohmeyer, D. Kuang, P. Wang, H.-W. Schmidt, S. M. Zakeeruddin and M. Grätzel, *J. Mater. Chem.*, 2006, **16**, 2978.
- 10 S. Chen, B. Zhang, N. Zhang, F. Ge, B. Zhang, X. Wang and J. Song, *ACS Appl. Mater. Interfaces*, 2018, **10**(6), 5871.
- 11 P. Chakraborty, S. Das and A. K. Nandi, *Prog. Polym. Sci.*, 2019, **88**, 189.
- 12 R. Bhandary and M. Schönhoff, *Electrochim. Acta*, 2015, **174**, 753.
- 13 A. Ikeda, K. Sonoda, M. Ayabe, S.-i. Tamaru, T. Nakashima, N. Kimizuka and S. Shinkai, *Chem. Lett.*, 2001, **30**, 1154.
- 14 Z. Qi, N. L. Traulsen, P. M. de Molina, C. Schlaich, M. Gradzielski and C. A. Schalley, *Org. Biomol. Chem.*, 2014, **12**, 503.
- 15 M. Bielejewski, *J. Sol-Gel Sci. Technol.*, 2018, **88**, 671.
- 16 T. Zhou, X. Gao, F. Lu, N. Sun and L. Zheng, *New J. Chem.*, 2016, **40**, 1169.
- 17 N. Kimizuka and T. Nakashima, *Langmuir*, 2001, **17**, 6759.
- 18 K. Hanabusa, H. Fukui, M. Suzuki and H. Shirai, *Langmuir*, 2005, **21**, 10383.
- 19 N. Minakuchi, K. Hoe, D. Yamaki, S. Ten-no, K. Nakashima, M. Goto, M. Mizuhata and T. Maruyama, *Langmuir*, 2012, **28**, 9259.
- 20 J. Yan, J. Liu, P. Jing, C. Xu, J. Wu, D. Gao and Y. Fang, *Soft Matter*, 2012, **8**, 11697.
- 21 T. Tu, X. Bao, W. Assenmacher, H. Peterlik, J. Daniels and K. H. Dötz, *Chem.–Eur. J.*, 2009, **15**, 1853.
- 22 L. Tan, X. Dong, H. Wang and Y. Yang, *Electrochem. Commun.*, 2009, **11**, 933.
- 23 X. Dong, H. Wang, F. Fang, X. Li and Y. Yang, *Electrochim. Acta*, 2010, **55**, 2275.
- 24 Y. Ishioka, N. Minakuchi, M. Mizuhata and T. Maruyama, *Soft Matter*, 2014, **10**, 965.
- 25 G. Sinawang, Y. Kobayashi, Y. Zheng, Y. Takashima, A. Harada and H. Yamaguchi, *Macromolecules*, 2019, **52**(8), 2932.
- 26 A. Maršavelski, V. Smrečki, R. Vianello, M. Žinić, A. Mogaš-Milanković and A. Šantić, *Chem.–Eur. J.*, 2015, **21**, 12121.
- 27 J. Makarević, M. Jokić, Z. Raza, Z. Štefanić, B. Kojić-Prodić and M. Žinić, *Chem.–Eur. J.*, 2003, **9**, 5567.
- 28 S. N. Denmark, R. A. Stavenger, A.-M. Faucher and J. P. Edwards, *J. Org. Chem.*, 1997, **62**, 3375.
- 29 E. O. Stejskal and J. E. Tanner, *J. Chem. Phys.*, 1965, **42**, 288.
- 30 L. Frkanec and M. Žinić, *Chem. Commun.*, 2010, **46**, 522.
- 31 M. Furlani, I. Albinsson, B.-E. Mellander, G. B. Appetecchi and S. Passerini, *Electrochim. Acta*, 2011, **57**, 220.
- 32 H. Tokuda, K. Hayamizu, K. Ishii, M. A. B. H. Susan and M. Watanabe, *J. Phys. Chem. B*, 2004, **108**, 16593.



- 33 H. Tokuda, K. Hayamizu, K. Ishii, M. A. B. H. Susan and M. Watanabe, *J. Phys. Chem. B*, 2005, **109**, 6103.
- 34 M. Moreno, M. Montanino, M. Carewska, G. Appetecchi, S. Jeremias and S. Passerini, *Electrochim. Acta*, 2013, **99**, 108.
- 35 G. Yu, X. Yan, C. Han and F. Huang, *Chem. Soc. Rev.*, 2013, **42**, 6697.
- 36 M.-O. M. Piepenbrock, G. O. Lloyd, N. Clarke and J. W. Steed, *Chem. Rev.*, 2010, **110**, 1960.